On the warm pool dynamics in the southeastern Arabian Sea during April – May 2005 based on the satellite remote sensing and ARGO float data

V. S. N. Murty*[a], S. Murali Krishna[b], A. Nagaraju[b], Y. K. Somayajulu[a], V. Ramesh Babu[a],
D. Sengupta[c], P. R. Sindu[c], M. Ravichandran[b], G. Rajesh[d]
[a]National Institute of Oceanography, Dona Paula, Goa, India
[b]Indian National Center for Ocean Information Services, Hyderabad, India
[c]Center for Atmospheric and Oceanic Sciences, Indian Institute of Science, Bangalore, India
[d]National Institute of Ocean Technology, Chennai, India.

ABSTRACT

Observational data from the Arabian Sea Monsoon Experiment (ARMEX-Phase IIA) in the southeastern Arabian Sea (SEAS) showed intense warming with the SST up to 31.5°C during April – May 2005. Analysis of 5–day repeat cycles of temperature and salinity profiles from an ARGO float (ID No. 2900345) in a 3°x1° box closer to ARMEX-II buoy (8.3°N, 72.68°E) in the SEAS during January – September 2005 revealed evolution of warm pool (SST>28°C) in spring 2005. The Argo data derived D20 (depth of 20°C isotherm) showed the influence of remote forcing during January – May, and local wind forcing during southwest monsoon. Low salinity waters (<34.0) occupied the top 30 m during January – February followed by temperature inversions (up to 0.5°C) in the 30-60 m depth range. From the peak spring warming, the SST dropped gradually by 3.5°C by end-July with the advent of southwest monsoon followed by a decrease in net heat gain upto 100 W/m². The merged weekly products of sea surface height anomalies and the NLOM simulated surface currents showed complex surface circulation consisting of seasonal Lakshadweep High/Low in winter/summer. The examined oceanic and atmospheric variables showed an intraseasonal variability with 41 to 63 day period, coinciding with the Madden-Julian Oscillation.

Key words: Southeastern Arabian Sea, ARMEX, Argo float, NLOM simulations, spring warm pool, heat budget, sea surface height anomaly, QuikScat winds and sea surface temperature

1. INTRODUCTION

Studies on the air-sea interaction of the Arabian Sea have been increased considerably with a special emphasis on the southeastern Arabian Sea (SEAS) processes since the time of identification of a large pool of warmer (>30°C) Sea Surface Temperature (SST) in the SEAS [1]. This large pool of warmer SST region since then is known as the Arabian Sea Warm Pool. The temperature of the warm pool (SST > 28°C) reaches up to 31°C [2] and can be seen in the climatological SST maps [3, 4] and in the SST maps derived using Tropical Rainfall Measuring Mission (TRMM) Micro wave Imager (TMI) satellite remote sensing images [5] and optimally interpolated weekly SST maps [6, 7]. It is reported that the Indian Ocean warm pool, which includes the SEAS warm pool, is much higher than in the Pacific Ocean [8]. Recently, an intense observational program, the Arabian Sea Monsoon Experiment (ARMEX), was conducted in the SEAS in two Phases (ARMEX-I: 15 June - 15August, 2002 and ARMEX-II: 14 March – 10 April and 15 May - 19 June, 2003) with an aim to understand the regional scale ocean-atmosphere coupled processes over the Arabian Sea, and to detail the growth and collapse of the warm pool in the SEAS [9]. The ARMEX data analysis reveals that the warm pool develops in the SEAS during March-April and intensifies to its maturity by May and collapses by June with the advent of the southwest monsoon winds and the associated air-sea interaction processes [10]. Various processes identifying the role of ocean in the genesis and annihilation of the core of the warm pool in the SEAS are reviewed by [7]. Several authors [5, 11, 12] analyzed the moored buoy observations and satellite remote sensing data during ARMEX-II to describe the characteristics of warm pool in the SEAS and the response of the SEAS to the local forcing. The impact of warm pool on the monsoon onset vertex in the SEAS was studied by [13]. Studies on development of Sea Surface

---

*vsnmurty@nio.org; phone +91 832 2450 460; fax +91 832 2450 608; www.nio.org

Remote Sensing of the Marine Environment, edited by Robert J. Frouin, Vijay K. Agarwal,
Hiroshi Kawamura, Shailesh Nayak, Delu Pan, Proc. of SPIE Vol. 6406, 640616, (2006)
0277-786X/06/$15 · doi: 10.1117/12.694254

Temperature High [6] and a mini warm pool [13] in the SEAS pointed out that the warm pool dynamics could be linked to the formation of the Lakshadweep High (LH) in the SEAS [14, 15]. Using the moored buoy temperature data from the SEAS, it is demonstrated that warming of the mixed layer is a response to net surface heat flux minus the penetrative solar radiation below the mixed layer [16]. Utilizing the Argo float measured temperature and salinity profiles in the SEAS, the seasonal cycles of temperature and salinity and the build-up of warm pool are demonstrated by [17]. It is reported that the build up of warm pool was associated with the occurrence of low sea surface salinity, and collapse of the warm pool was associated with the occurrence of high salinity waters [17]. The above studies are carried out using shorter time series data colleted during field experiments and based on the numerical model simulations. The advent of Argo float measured temperature and salinity profiles gives an opportunity to study the upper ocean variability on intraseasonal to seasonal time scales. In order to understand the role of advection in the mixed layer heat budget in the SEAS, a third observational program, the ARMEX-IIA, was launched during 15 April – 6 May 2005 by the Department of Science and Technology (DST), New Delhi to measure time series of currents through current meters attached at 2 m, 7 m, 15 m and 25 m depths to the surface moored buoy which also facilitates simultaneous measurements of surface meteorological parameters. In this study, we present the temporal variability of warm pool in the SEAS based on ARMEX-IIA observations (15 April – 5 May, 2005) and seasonal evolution of warm pool and upper ocean heat budget in 2005 in the SEAS through a single ARGO float data from January to September 2005. The dynamics associated with the warm pool evolution are discussed based on surface circulation derived from weekly merged TOPEX/POSEIDON, Jason and ERS-1/2 Sea Surface Height Anomalies (SSHA) and the 1/16° global Naval Research Laboratory (NRL) Layered Ocean Model (NLOM) simulated daily averaged surface currents during January – September, 2005.

2. OBSERVATIONS AND REMOTE SENSING DATA

We used the SBE (SeaBird Electronics Ltd, US make) Seacat CTD (Conductivity-Temperature-Depth probe) temperature and salinity profiles data in the upper 500 m collected during 15 April – 5 May, 2005 in the SEAS under the ARMEX-IIA program at a stationary location of the ARMEX-IIA moored buoy (8.2°N, 72.68°E) and also along two short sections (about 300 km length) from the buoy to Indian (Kochi) coast (Fig. 1a). The Seacat CTD salinity was corrected using a regression line obtained between the pairs of CTD salinity and Autosal salinity data. Time series of Seacat CTD were obtained at 5 locations (of 13 km apart from the central location (8.3°N, 72.68°E) of the ARMEX-moored buoy). The stationary buoy location is shown by open circle in Fig. 1a. The rectangle in Fig. 1a represents the area within which an ARGO float (ID No. 2900345) moved during 1 January – 30 September 2005, providing an opportunity to study the seasonal evolution of the warm pool in the SEAS, and its track is shown in Fig. 1b.

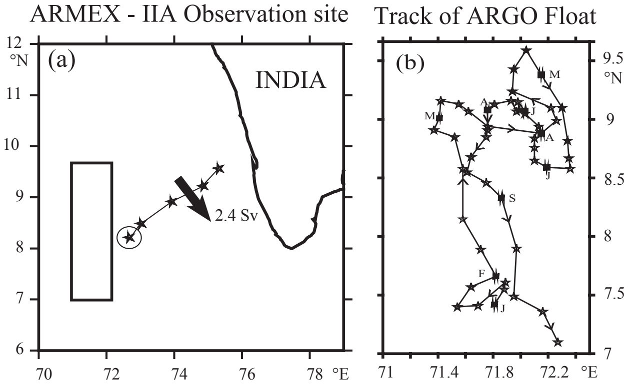

Fig. 1. Study area showing (a) ARMEX-IIA observation site (○) and CTD stations (*) occupied during 15 April – 5 May, 2005 in the southeastern Arabian Sea. The bold arrow in (a) represents the geostrophic volume transport (2.4x106 m3/s towards southeast) in the upper 300 m across the section during 19-21 April 2005. The rectangle in (a) corresponds to the area (3°x1°) tracked by an Argo float (ID No. 2900345) and (b) the locations of the 5-day repeat cycles of the Argo float during January – September 2005. The alphabets in (b) represent the float location at the start of each month.

The Argo float moved northward from 7.3°N in January and remained almost stationary from March to August around 9°N and reached back to 7°N by 30 September. The mixed layer depth is obtained from temperature criterion – the depth at which the water temperature is 1°C less to the SST (MLD-T) and density criterion – depth at which the water density

(Sigma-theta) is higher by 0.125 from sea surface density (MLD) [18, 19]. The difference between MLD-T and MLD is termed as the Barrier Layer Thickness (BLT). The closest depth of temperature and salinity nearer to the sea surface is 2 m in case of Seacat CTD and Buoy data and 4 m in case of Argo float data. The net heat flux at sea surface is estimated from the ARMEX moored buoy measured surface meteorological data including solar radiation, longwave radiation, relative humidity, air temperature, SST (at 2 m depth) and wind speed and direction.

We also made use of the 'Adjusted' Southampton Oceanographic Center (SOC) climatology [20] (http://**www.soc.soton.ac.uk/JRD/MET/Fluxclimatology.php**), National Center for Environmental Prediction/National Center for Atmospheric Research (NCEP/NCAR) climatology [21] and Ocean Atmosphere Flux (OAFLUX) climatology [22] (**http://oaflux.whoi.edu/data.html)** on monthly mean data of air-sea heat fluxes (latent and sensible heat), solar radiation, longwave radiation and net heat flux at the grid point close to ARMEX buoy location (8.2°N, 72.68°E) in the SEAS during January – December 2005. The Tropical Rainfall Measuring Mission (TRMM) Micro wave Imager (TMI) satellite remote sensing images [23] derived weekly SST maps from April to May 2005 are used. The upper ocean heat content [24] is computed in different layers (0-10 m, 0-20m, 0-40 m, 0-60 m and 0-100 m) and also in the slabs of 15 m, 20 m and 25 m thick in the upper 200 m at the locations of ARMEX-IIA program (20 April – 4 May, 2005) and also using the 5-day repeat Argo float temperature profiles in the SEAS (Fig. 1b) from January to September 2005. The gridded product of merged TOPEX/POSEIDON, JASON-1 and ERS-1/2 remote sensing satellites derived weekly SSHA data [25] (http://**www.aviso.oceanobs.com**) during 1997-2005 are used to estimate the geostrophic velocity field at sea surface. The NLOM simulated daily surface current vectors [26] (**http://www7320.nrlssc.navy.mil/global_nlom)** are also used to describe the sea surface circulation for the observational period in the SEAS. The weekly SSHA data for the 9 years period (1997-2005) have been low pass filtered with a period ≥90 day to obtain seasonal harmonic and band pass filtered with 20-90 day period to obtain intraseasonal harmonic. FFT analysis [27] was also carried out to identify the dominant periods in the low pass filtered and band pass filtered time series data of SSHA, TRMM SST, Argo float derived parameters - heat content (HC) and depth of 20°C isotherm (D20).

3. RESULTS AND DISCUSSION

3.1 Upper ocean variability in the SEAS from ARMEX-IIA observations

Figs. 2a-b show the variation of temperature and salinity measured at 2 m and 7 m depths at the ARMEX buoy location during 21 April – 4 May 2005. One can see gradual build up of warm pool with highest temperature (>31°C) from 21 April to 1 May, followed by abrupt decrease. One can also see the large temperature difference between 2 and 7 m depths during the warming period. The salinity variation shows occurrence of high and low salinity waters with a 7 day duration. Relatively low salinity (34.3 and 34.45) waters occurred on 26 April. As warm pool builds up the near-surface salinity also increased. The Argo float measured SST (at 4 m depth, Fig. 2c) shows the gradual evolution of warm pool from 28.5°C on 1 March to a peak value of 31.2°C by end of May. The TMI SST (Fig. 2c) closely follows that of Argo SST, though some deviations can be seen on 3 occasions (mainly due to differences in the depth of sampling). The WOA01 climatological monthly SST falls within the curves of Argo SST and TMI SST, but showed wide variation from May to October. The climatological maximum SST was 29.5°C, about 2° less than the observed values in the warm pool area. The curves of Argo SST and TMI SST showed a gradual fall by 3°C from June to beginning of August, the period of southwest monsoon. During August – October, the SST curves showed a slight rise by 1°C, with the retreat of the southwest monsoon winds from the SEAS. The SST pattern shows the weak bimodal variation [28]. The secondary warming during August-October is resulted from the slight increase in solar radiation due to cloud-free conditions after the southwest monsoon. A slight cooling in SST can also be seen in September, may be associated with an intraseaonsal event. The warm pool build up can be seen till the end of May in the Argo data than in the buoy measurements (Fig. 2a). This may be due to spatial difference in the location of Argo float and the ARMEX moored buoy (Fig. 2a). The warm pool SST in May 2005 is higher by 1°C than that in May 2003 [7], indicating the interannual variation. The Argo SSS (at 4 m depth) shows a variation of low salinity waters (<34.0) in January and high salinity (>36.4) in the first week of September. The Argo SSS also increased gradually during the warm pool build up. The Argo SSS in May is similar to that measured at the moored buoy location, and that reported by [7] in 2003. The Argo annual surface salinity variation with low salinity in January – February and high salinity in August – September can be linked to the annual variation of surface currents in the SEAS (discussed in section 3.3).

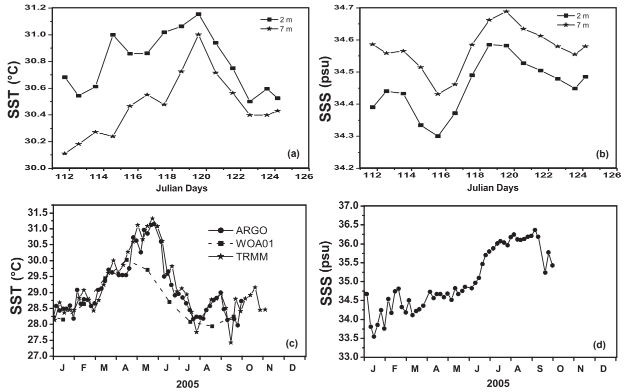

Fig. 2. Time variation of daily averaged near-surface parameters (a) temperature (°C) and (b) salinity (psu) at 2 m and 7 m depths at the ARMEX-IIA moored buoy (8.3°N, 72.67°E) during 21 April – 4 May, 2005 and of annual variation of Argo float measured (5-day repeat cycle) near-surface parameters (c) temperature (°C) and (d) salinity (psu) during January – September 2005 in the SEAS. Also included in (c) are the World Ocean Atlas 2001 archived climatological SST (°C) and TRMM/TMI SST (°C) averaged over the Argo float tracked area (3°x1°) as shown in Fig. 1.

Figs. 3a-c represent the upper ocean (0-200 m) thermal, salinity and density structures at the central location (8.3°N, 72.67°E) during 26 April - 4 May 2005 during ARMEX-IIA. The central location was closer to the ARMEX-IIA buoy located off Minicoy Islands. A thin (~25 m) warm (>30°C), less saline (<34.7) and less density (<21.5 sigma-theta) layer, constitutes the boreal spring 'Warm Pool' in the SEAS. The thermocline (between 28°C and 16°C isotherms) is evident between 75 and 150 m depth. In the mid-thermocline, a subsurface high salinity (35.3 - 35.4) watermass is embedded.

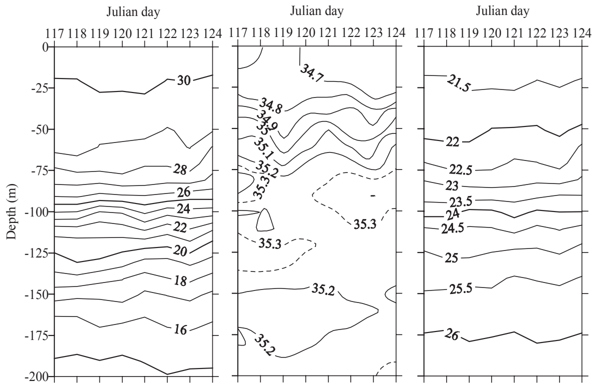

Fig. 3. Time-depth sections of (a) potential temperature, (b) salinity and (c) potential density at the time-series central location (8.3°N, 72.67°E) during ARMEX-IIA observation period (26 April – 4 May 2005) in the SEAS.

Figs. 4a-c and 5a-c represent the upper ocean (0-200 m) thermal, salinity and density structures along the short sections (300 km) from the ARMEX buoy to off the Indian (Kochi) coast during 19 – 20 April and during 5-6 May respectively. In April, the warm pool characterized by warmer temperature (>30°C), low salinity (<34.8) and less dense (<21.5 sigma-theta) water occupies the upper 20 m. The thermocline (16°-28°C) is characterized by the subsurface high salinity (35.3-35.9) watermass with its core located closer to the Kochi coast. In May, the warm pool deepened up to 30 m and intensified with an increase in temperature by 1°C and salinity by 0.2. The upper 30 m layer is occupied by low density (<21.5 sigma-theta) waters. The subsurface salinity maximum is seen separated into cells of high salinity. The isotherms, isohalines and isopycnals exhibited downward sloping above 100 m and upsloping below 100 m depth, on the eastern side of the section (towards Kochi coast).

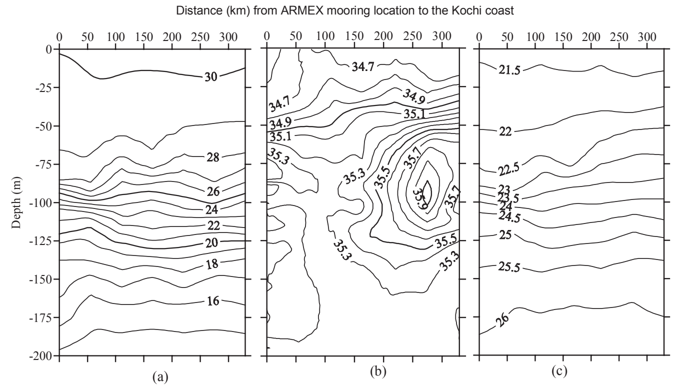

Fig. 4. Distance-depth sections of (a) potential temperature, (b) salinity and (c) potential density along the section from ARMEX-IIA moored buoy to Kochi coast during 19 – 21 April 2005.

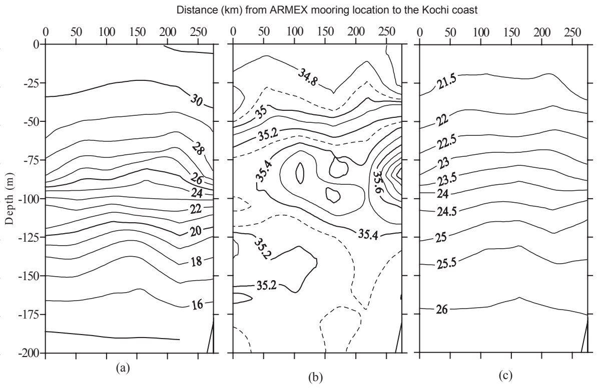

Fig. 5. Same as in Fig. 4, but during 5 – 6 May, 2005

3.2 Upper ocean variability from ARGO float data

Figs. 6a-b show the upper ocean (0-200 m) thermal and salinity structures as derived from the Argo float data during January – September 2005 in the SEAS. The Argo data provided an opportunity to study the seasonal cycle of temperature and salinity together with the evolution of warm pool in this region. In January – February, the SST is about 28.5°C followed by subsurface inversions of about 0.5°C between 40 and 60 m depth. The magnitude of inversion agrees well with the climatological model simulation of [29]. Westward propagation of the temperature inversions with the westward annual Rossby waves is reported by [30]. The time and spatial variation of temperature reveals the bowl shape of the spring warm pool (of temperature >29°C) in 2005. The warm pool began in March and persisted till June, and the base of the warm pool varied between 30 to 50 m at its peak intensity of highest SST (>30-31°C) in May 2005. The near-surface layer (up to 30-40 m depth) temperature was about 0.5°-0.7°C less prior to the development of warm pool and soon after its collapse after 15th June. The decrease in the surface layer temperature is due to the southwest monsoon wind mixing and abrupt decrease in the net heat gain (of the previous months) across the air-sea interface. The isotherms in the thermocline exhibited upward and downward undulations at intraseasonal scale. The cooling of the surface layer after 15th June might also be due to the upward movement of the thermocline in June. Lowest salinity (<34.2) waters are seen in end-January and agree well with the observed salinity (34.2 – 34.3) along the XBT tracklines in the SEAS (see Fig. 3f in [30]).

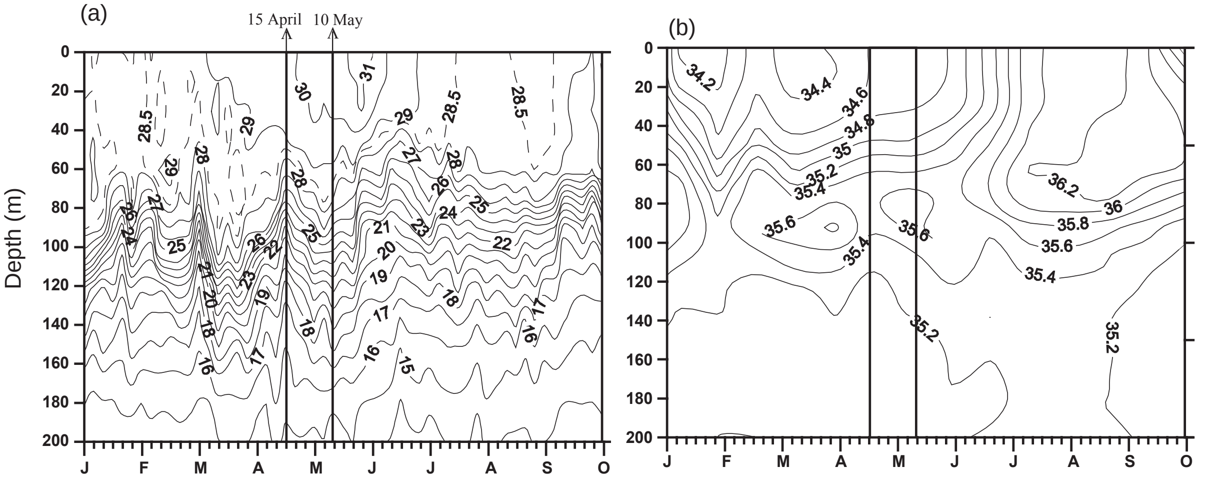

Fig. 6. Time-depth sections of upper ocean (a) thermal structure and (b) salinity structure derived from the Argo float data during January – September 2005. The vertical box represents the ARMEX-IIA observation period.

From February to June, a subsurface high salinity maximum (35.4 – 35.6) is embedded in the thermocline between 70 and 120 m depth. In the top 70 m layer, the salinity increased gradually from February till June. Coinciding with the upward rise of the thermocline in June, the upper part of the subsurface high salinity layer also rises to the sea surface and the isohalines show a well- mixed layer. From mid-June to end September, very high salinity (36.2) waters occupied the upper 80 m layer, and the subsurface salinity maximum was absent. These high salinity waters in the upper 80 m layer have their source in the northern Arabian Sea and flowed equatorward off the west coast of India through the equatorward flowing West India Coastal Current (WICC) [7]. The salinity structure points out a 2-layer flow pattern from February to June: westward/northwestward flow in the top layer (0-60 m) encompassing the warm pool (>29°C) and eastward/southeastward subsurface flow centered around 100 m depth, below the base of the warm pool. From mid-June to September, the 2-layer flow pattern is replaced by a single layer flow in the upper 120 m. The poleward flow during winter (the WICC) from the southeastern region of the SEAS brings in low salinity waters of the Bay of Bengal origin [7].

Fig. 7 represents the variation of mixed layer depth (obtained with the temperature criterion (MLD-T) and density criterion (MLD) and barrier layer thickness (BLT, obtained as the difference in the mixed layer depths) derived from Argo data during January – September 2005. During January to mid-April, the MLD-T shoaled from 100 m to 50 m and during mid-June to September, it varied between 50 and 70 m. However, the MLD-T exhibited intraseasonal variation, particularly during January to April. The MLD varied between 8 and 35 m during the year, though intraseasonal variation is evident from January to June. The MLD is very shallow (5 m) on 15 September. During mid-April to mid-June, the MLD-T varied between 28 m and 42 m and the MLD varied between 8 m and 28 m. The shallow MLD during January to mid-April is associated with the capping of low salinity waters in the upper 30 m (Fig. 6b). The low salinity waters, which are of Bay of Bengal origin, are advected into the SEAS by the poleward flowing WICC [7]. Though the surface layer temperatures are low, the overlying low salinity waters develop a stratified water column in the upper 30 m and inhibit mixing due to entrainment.

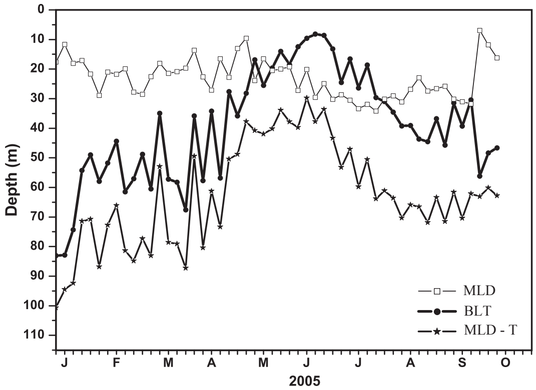

Fig. 7. Time-depth section Argo float data derived mixed layer depth (m) based on temperature criterion (MLD-T), density criterion (MLD) and the barrier layer thickness (BLT) during January – September 2005.

The prevailing relatively large negative wind stress curl field during January – March, however, suggests sinking process during this period. During May – July, the BLT variation is interesting. The BLT gradually decreased from 38 m from mid-April to 8 m by 10th June with the development of warm pool followed by the start of subsurface upwelling process with the southwest monsoon wind forcing (discussed further in the preceding sections). During this period, the MLD deepened from 8 m to 30 m, due to intense mixing associated with the monsoon wind forcing. While MLD deepened due to mixing in the surface layer, the MLD-T shoaled up due to curl induced upwelling, and both processes led to decrease of BLT.

3.3 Surface circulation variability from T/P SSHA data and model simulations

The variations in mean dynamic heights at the 5 time-series locations centered around the ARMEX moored buoy (Fig. 2) suggested a southward pressure gradient (2 dyn. cm over a distance of 26 km between N and S locations), which would support a westward geostrophic current. Figs. 8a-b show the geostrophic current structure along the shorter section (Fig. 3a) during 19-21 April and geostrophic velocity profiles between the station pairs on the return shorter section (Fig. 4a) during 4-5 May. The current structure shows the predominant southeastward current (12 cm/s) and a weaker northwestward flow towards Kochi coast. The southeastward flow in April intensified (18 cm/s) at surface by May and a flow reversal towards northwest took place at around 100 m depth (Fig. 8b). The mean volume transport is about 2.4 x 10^6 m^3/s (depicted by an arrow in Fig. 1a).

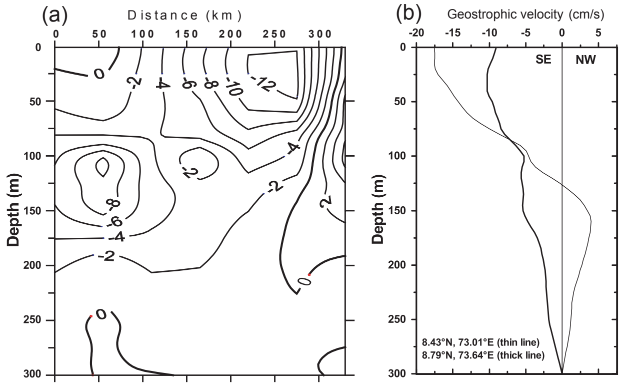

Fig. 8. (a) Distance – depth section of geostrophic current (cm/s) structure in the upper 300 m along the section from the ARMEX-IIA moored buoy to Kochi coast during 19 – 21 April 2005. Southeastward flow (negative velocity contours) is dominant across the section, and (b) velocity profiles between two station pairs during 5 - 6 May 2005.

The weekly SSHA averaged in the Argo float tracked area is shown in Fig. 9a for the period of January – September 2005. In this grid, the SSHA is large +10 cm in first week of January and -18 cm in the first week of July. During the development of warm pool (March – May) and during southwest monsoon period (September), the SSHA is weakly positive reaching up to 2-3 cm, depicting intraseaonal variability in the SSHA in the SEAS. While the large positive SSHA corresponds to the LH, the large negative SSHA in early July corresponds to the Lakshadweep Low (LL) [7, 14]. Fig. 9b represents the weekly variation of the SSHA derived zonal (u_g) and meridional (v_g) component of geostrophic velocity during January – September 2005 at the ARMEX moored buoy in the SEAS. A northwestward flow occurs during January – March, corresponding to the poleward flow of the LH, while the southeastward flow during mid-May – September is associated with the LL. The variations in the u_g and v_g are due to the flows associated with the westward movement of the LH and LL. The large westward flow in December marks the beginning of the northwestward flow associated with the LH.

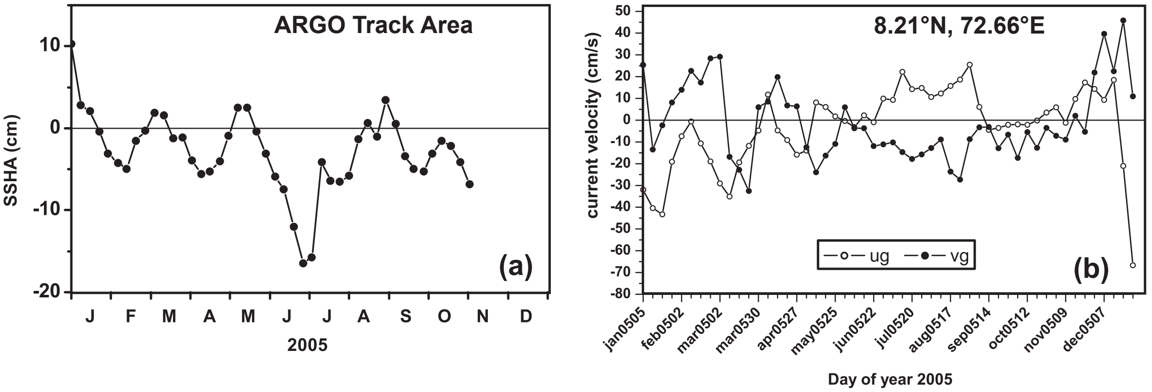

Fig. 9. Temporal variation of (a) weekly merged SSHA (cm) averaged over the Argo float tracked area (3°x1° box shown in Fig. 1) during January – October 2005, and (b) weekly geostrophic zonal (u_g) and meridional (v_g) currents derived from merged SSHA data at ARMEX-IIA buoy location (8.21°N, 72.66°E) during January – December 2005.

Thus the annual variation of currents in the SEAS is dominated by the presence of LH and LL and their westward movement due to the propagation of radiated Rossby waves off the west coast of India. The evolution of SSHA and the associated geostrophic surface circulation during the warm pool development period (April – May 2005) is shown in Figs. 10a-d. The ARMEX moored buoy is depicted as '+' in Figs. 10a-d. The surface circulation is characterized with a number of anticyclonic and cyclonic meso-scale eddies. The growth and westward movement (about 6 to 11 cm/s) of these eddies is also evident. On 27th April, one can see large scale northwestward flow in the open sea and southeastward flow off the Indian coast constituting the large band of anticyclonic flow, embedded in it is the LH centered at 9°N, 73°E. These meso-scale eddies give rise to the intraseasonal variation in the SSHA and the derived geostrophic currents.

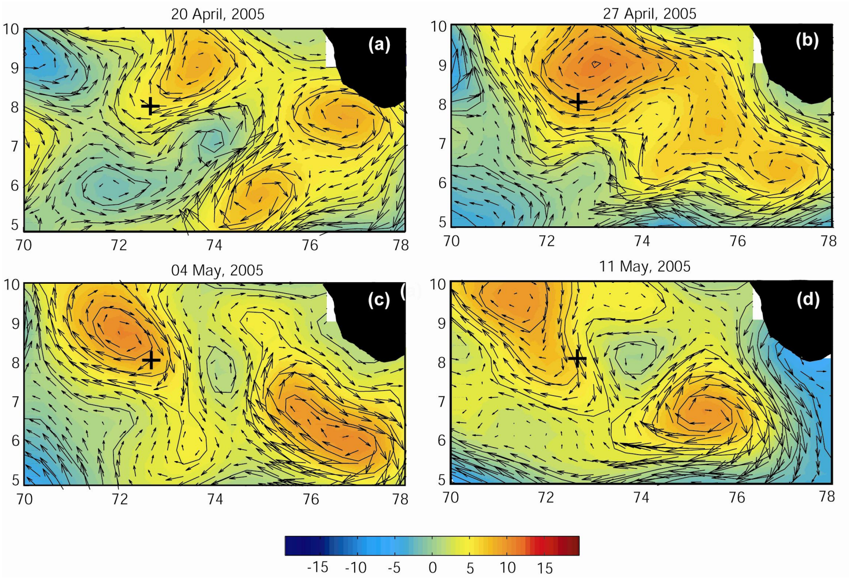

Fig. 10. Evolution of weekly merged SSHA (cm) during (a) 20 April, (b) 27 April, (c) 4 May and (d) 11 May, 2005 in the SEAS. Superimposed are the geostrophic current vectors depicting the surface circulation.

Figs. 11a-d represent the interannual variation of the SSHA in the 3°x3° grid (7-10°N and 70-73°E) during 1997 – 2005. In these figures, each minor tick on the abscissa indicates a duration of 2 months. There occurs interannual variation only in the positive SSHA particularly in 1997-98, 2001 and 2003 when the SSHA is relatively less, compared the values in the other years. Negative SSHA is relatively less in October – November 1997, corresponding to the 1997-98 Indian Ocean Dipole Mode event [31, 32].

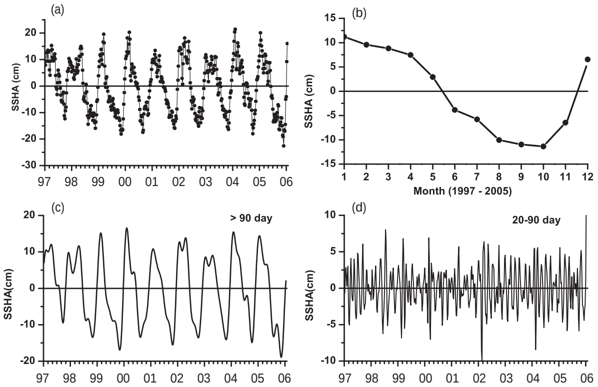

Fig. 11. (a)Interannual variation of weekly SSHA (cm) during 1997 – 2005, (b) 9 year mean annual variation of SSHA, (c) interannual variation of low pass filtered (> 90 day) SSHA and (d) interannual variation of band pass filtered (20 - 90 day) SSHA, at the ARMEX- IIA buoy location (8.3°N, 72.68°E).

The annual variation of 9 year mean monthly SSHA (Fig. 11b) obtained from the data in Fig. 11a clearly depicts the seasonal variation in SSHA – positive during December – May, the period of warm pool development and LH formation, and the negative SSHA between June and September constitutes the growth and development of LL. The weekly SSHA as in Fig. 11a is subjected to the FFT analysis with a 90 day period low pass filtering, and the resultant time variation of low pass filtered SSHA is shown in Fig. 11c. One can see the seasonal peaks of SSHA representing the LH during March – April, with interannual variation in SSHA in 2003 with lower (+8 cm) value and relatively large SSHA (+16 cm) in 2000. Similarly the negative SSHA associated with the LL is large in 1999 (-18 cm) and in 2005 (-20 cm). The amplitude of interannual variation is about 15 cm. Fig. 11d represents the band pass filtered (20-90 day period) SSHA showing the intraseasonal variation of SSHA of amplitude varying between ±10 cm. The intraseasonal peaks (both positive and negative) occurred at a lag of 2 months from the seasonal peaks (>90 day period, Fig. 11c). The intraseasonal peaks are large in March 2002 and December 2005. Fig. 11d suggests that the intraseasonal peak has a period of 50-60 day, the Madden Julian Oscillation (MJO). This intraseasonal variability in the sea surface height might be resulted from the intraseasonal variability in the net heat flux (due to heat fluxes which depend on wind speed) or of the upper ocean heat content in the SEAS. The seasonal variability in the upper ocean heat content in the SEAS might result from the seasonal circulation dominated by the LH and LL. The NLOM simulated daily surface currents in 5-day intervals are examined for January, April, May and August, 2005 representing the winter monsoon, spring warm pool development period (April – May) and summer monsoon seasons, and presented only for January and May (Figs. 12a-d). These high resolution surface currents at 1/16° grids show intense intraseasonal variability in the surface currents consisting of a numerous meso-scale eddies of anticyclonic and cyclonic circulation. At the boundaries of eddies, one can see a strong current shear and also the broad currents encompassing them. One can see a developed LH between 7.5°N and 10°N and between 71°E and 73.5°E by 15 January 2005 (Fig. 12b), and all the eddies formed in the eastern of the study area off the southwest coast of India and moved westward in time. By May, the LH has grown and moved towards west. The LH is surrounded by smaller scale eddies. Westward shift of the LH associated with the westward propagation of annual Rossby wave, radiated from the southwest coast of India, was reported [14]. By 15 May (Fig. 12d), a southeastward flow is set in off the Indian coast. Along with this flow, the northern Arabian Sea high salinity waters also get advected into the SEAS, which is evident from the Argo float salinity structure (Fig. 6b).

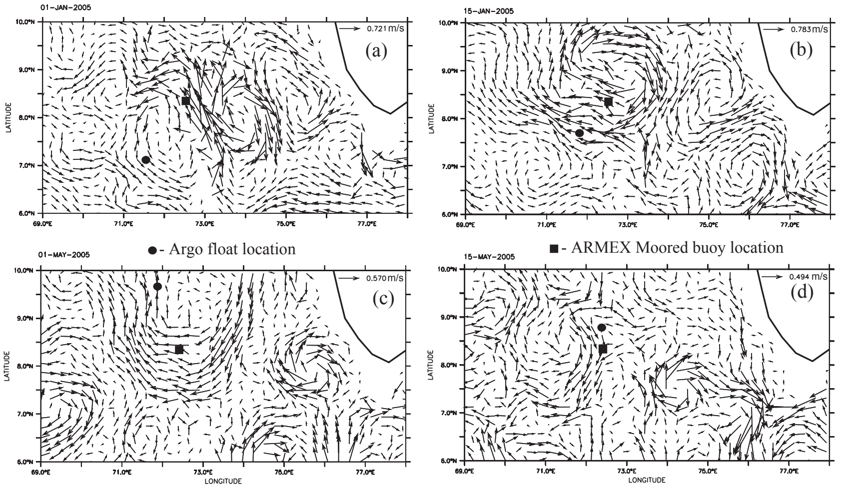

Fig. 12. NLOM simulated surface currents in the SEAS (a & b) during winter (1 and 15 January) and (c & d) during summer (1 and 15 May). The symbols (● and ■) denotes Argo float location on the day of simulation and the ARMEX – IIA buoy location.

3.4 Net heat flux and upper ocean heat content variability

The ARMEX moored buoy measured surface meteorological parameters at 3 hourly intervals are utilized to compute the air-sea heat fluxes (latent heat and sensible heat) and net heat flux (incoming solar radiation – longwave radiation – latent heat flux – sensible heat flux) at the mooring location (8.3°N, 72.68°E) during 21 April – 4 May (Fig. 13a).Throughout this period, the net heat flux is positive indicating that the sea surface gained heat during this observational period. In April, the average net heat flux is about +90 W/m² and in May (4 days average) it is about +30 W/m². The three climatological monthly mean data sets (SOC, NCEP/NCAOR and OAFLUX) showed a difference of about 10 W/m² and OAFLUX latent heat flux is lower compared to the other 2 data sets. This has caused the OAFLUX net heat flux to be less by 10-20 W/m² compared to SOC and NCEP/NCAR (Fig. 13b). The annual variation of net heat flux shows heat gain at sea surface with a maximum of 100 W/m² in March and September and minimum of 5 W/m² in June. From March to May, the period of warm pool development, the net heat gain gradually decreased with the advent of southwest monsoon bringing in high cloud amounts and strong winds and the associated increase of latent heat flux. The upper ocean heat content (HC) in slabs of 20 m is estimated from Argo temperature data from January – September 2005 (Fig. 14a). The HC in 0-20 m slab is minimum (23.5×10^{8} J/m²) in the first week of January and increased steadily to a maximum of (25.5 x10^8 J/m²) by end May in accordance with annual march of the Sun north of equator during which period the sea surface gains heat across air-sea interface and the warm pool develops in the SEAS. The HC drops steadily to a lower value by end July from the peak value with the beginning and strengthening of the southwest monsoon winds leading to a rapid decrease in net heat gain (Fig. 14a) and from the surface layer. The 0-20 m lost more heat by end-July compared to the lower value in January. This is due to the occurrence of subsurface temperature inversions in January and February from 15 m to 50 m and layer cooling due to net heat loss from the sea surface and also by the upwelling of cold waters from below towards the surface during southwest monsoon months.

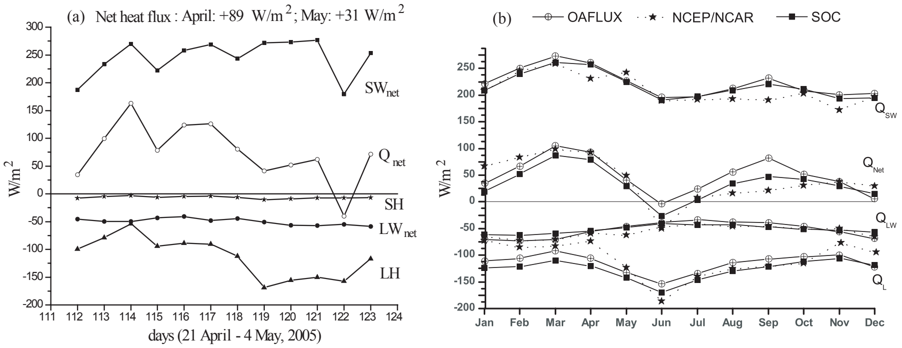

Fig. 13. Temporal variation of heat budget parameters and net heat flux (a) during ARMEX - IIA observation period (21 April – 4 May, 2005) and (b) based on Monthly climatology of SOC, NCEP/NCAR and OAFLUX.

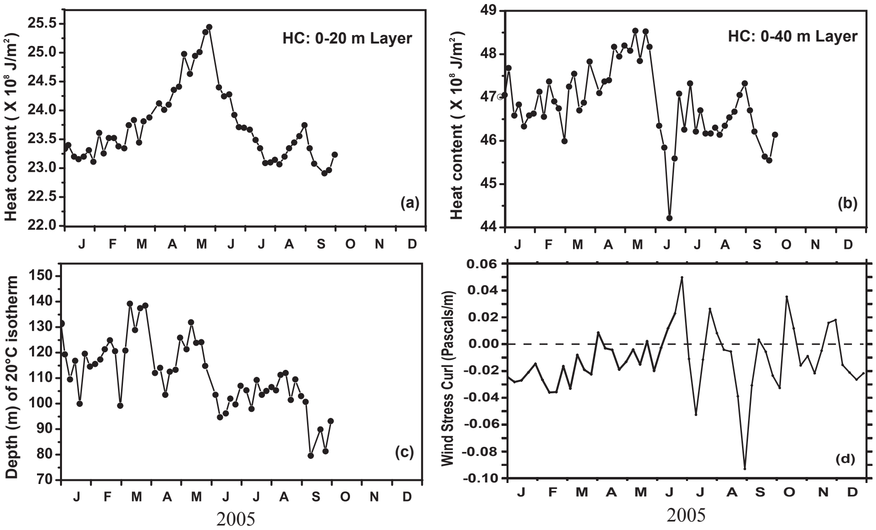

Fig. 14. Monthly variation of (a, b) upper ocean heat content in 0-20 m layer and 0 – 40 m layer, (c) depth of 20°C isotherm and (d) wind stress curl.

This suggests that vertical advection process is important to the upper layer heat budget in the SEAS. The HC is increased during August and decreased by same magnitude in September. The HC in the 0-40 m layer (Fig. 14b) shows warming from January to mid-May as warm pool developed, and abrupt loss of heat from mid-May to mid-June marking the intense upwelling of cold waters from 40 m and below due to Ekman pumping during the southwest monsoon. From mid-June to early July, the HC in 0-40 m layer increased sharply and maintained the same HC till September. The HC from mid-June to end September period is relatively lower (46.5 x10^8 J/m²) compared to that during January to May. The former represents the development and persistence of LL while the latter the period of LH development. The annual variation in the depth of 20°C isotherm (D20) suggests intraseasonal variability (Fig. 14c) and this D20 variation is also reflected in the HC variation in 0-40 m layer. The annual variation of averaged wind stress curl in the Argo float track area shows weaker downwelling during January – May and intense upwelling and downwelling beyond May (Fig. 14d). This variability in the Ekman pumping velocity affected the HC in the 0-40 m layer. The large drop in HC in 0-40 m layer in June is resulted mainly from the intense upwelling in June, marking the beginning of LL formation. The prevailing negative wind stress curl during July and August did not show any influence either on D20 or HC (0-40 m layer). However, the reduction in the negative curl field in September caused shoaling of the D20 and resulted in the drop in HC (0-40 m layer). The FFT analysis of band pass filtered (20-90 day period) SSHA, Argo SST, TRMM/TMI SST, HC (0-20 m), D20 and wind stress curl revealed the presence of dominant spectral peaks between 41 and 63 days, coinciding with the Madden-Julian Oscillation (MJO) period [33]. It is reported that the atmospheric pressure at the coastal stations on the west coastal of India exhibit a dominant mode with 60-70 day period during January – March, whereas it shifts to 56-60 day period after May, during which period 30-40 day mode is prominent [34]. The FFT analysis of the above variables when low pass filtered with >90 day period revealed the dominant annual and semi-annual peaks besides a peak at around 120 day.

4. CONCLUSIONS

We have made use of the *in situ* time series of ocean observations carried out during ARMEX-IIA program and also the long term *in situ* temperature and salinity profiles obtained from a single ARGO float to understand the temporal upper ocean variability in the SEAS. In order to understand the dynamics associated with the warm pool development (March – May) and its collapse (May – July) with the southwest monsoon season, we have used the satellite remote sensing data on various parameters including the SSHA, SST and surface winds and wind stress curl. We have also used the NLOM simulations on the surface currents to describe the circulation variability in the SEAS. Near-surface T and S identified the spring warm pool and bowl of fresh water. The rate of HC change in the 0-20 m (40-60 m) slab showed heat gain of 52 W/m² (-25 W/m²) during March – May and heat loss of -40 W/m² (-68 W/m²) during May – June, in association with the development and collapse of spring warm pool and the simultaneous occurrence of LH and LL respectively. It is revealed that the upper ocean heat content variability in the SEAS is related both to the seasonal variation of sea level (LH and LL) and also to the intraseasonal variability between 41 and 63 day period in the oceanic and atmospheric (wind stress curl) parameters.

ACKNOWLEDGEMENTS

The authors are thankful to their Directors for encouraging a collaborative study under the national program of the Arabian Sea Monsoon Experiment (ARMEX-IIA). The ARMEX-IIA program was launched and funded by the Department of Science and Technology (DST), New Delhi as a part of the Indian Climate Research Program (ICRP). The Ministry of Ocean Development funded the national ARGO program under which Argo floats were deployed in the tropical Indian Ocean including the southeastern Arabian Sea. This is the NIO contribution No. XXXXX.

REFERENCES

1. P.V. Joseph, “Warm pool over the Indian Ocean and monsoon onset.” *Trop. Ocean Global Atmos. Newsl.*, **53**,1-5 (1990).
2. K.V. Sanilkumar, P.V. Hareesh Kumar, Jossia Joseph and J.K. Panigrahi, “Arabian Sea mini warm pool during May 2000.” *Current Sci.*, **86**, 101-105(2004).
3. S. Hastenrath, and P.J. Lamb, *Climatic atlas of the Indian Ocean Part I: Surface climate and atmospheric circulation*. Univ of Wisconsin Press, Madison, USA. Carts: 1-94(1979).
4. S. Levitus and T.P. Boyer, *World Ocean Atlas 1994*. Vol. 4: Temperature, NOAA Atlas NESDIS 4, US Department of Commerce, Washington DC (1994).
5. P.V. Hareesh Kumar, P. Madhusoodanan, M.P. Ajai Kumar and A. Raghunadha Rao, “Characteristics of Arabian Sea mini warm pool during May 2003.” *Mausam*, **56(1)**, 169-174(2005).
6. S.S.C. Shenoi, D. Shankar and S.R. Shetye, “The sea surface temperature high in the Lakshadweep Sea before the onset of the southwest monsoon.” *J. Geophys Res.*, **104**, 703-712(1999).
7. S.S.C. Shenoi, D. Shankar, V.V. Gopalakrishna and F. Durand, “Role of ocean in the genesis and annihilation of the core of the warm pool in the southeastern Arabian Sea.” *Mausam*, **56(1)**, 147-161 (2005).
8. P.N.Vinayachandran and S.R. Shetye, “The warm pool in the Indian Ocean.” *Proc Indian Acad Sci.*, **100**, 165-175(1991).
9. P. Sanjeeva Rao, “Arabian Sea monsoon experiment: An overview.” *Mausam*, **56(1)**, 1-6 (2005).

10. C. Gnanaseelan, Bijoy Thompson, J.S. Choudary and P.S. Salvekar, "Evolution and collapse of Arabian Sea warm pool during two contrasting monsoons 2002 and 2003." *Mausam*, **56(1)**, 187-200 (2005).
11. K. Jossia Joseph, M. Harikrishnan, G. Rajesh and K. Premkumar, "Moored buoy observations in Arabian Sea warm pool." *Mausam*, **56(1)**, 161-168(2005).
12. J. S. Chowdary, C. Gnanaseelan, Bijoy Thompson, S.K. Sinha and P.S. Salvekar, "Response of Arabian Sea to the local forcing during 2003 pre-monsoon warming phase." *Mausam*, **56(1)**, 175-186 (2005).
13. R.R. Rao and R. Sivakumar, "On the possible mechanism of the evolution of a mini warm pool during the pre-summer monsoon season and the onset vortex in the southeastern Arabian Sea." *Q. J. R. Meteorol. Soc.*, 125, 787-809 (1999).
14. D. Shankar and S. R. Shetye, "On the dynamics of the Lakshadweep high and low in the southeastern Arabian Sea." *J. Geophys. Res.*, 102(6), 12551-12562 (1997).
15. J. G. Bruce, J.C. Kindle, L.H. Kantha, J.L. Kerling and J.F. Bailey, "Recent observations and modeling in the Arabian Sea Laccadive High region." *J. Geophys. Res.*, **103**, 7593-7600 (1998).
16. D. Sengupta, P.K. Ray and G. S. Bhat, "Spring warming of the eastern Arabian Sea and Bay of Bengal from buoy data." *Geophys. Res. Lett.*, **29**, doi:10.1029/2002GL015340 (2002).
17. M. Ravichandran, P.N. Vinayachandran, S. Joseph and K. Radhakrishnan, "Results from the first Argo float deployed by India." Curr Sci., 86, 651-659(2004).
18. B. A. Kara, P.A. Rochford, H.E. Hurlburt, "Mixed layer depth variability over the global ocean." *J. Geophys. Res.*, **108(C3)**, doi:10.1029/2000JC000736 (2003).
19. T.V.S. Udaya Bhaskar, D. Swain and M. Ravichandran, "Inferring mixed layer depth variability from Argo observations in the western Indian Ocean." *J. Mar. Res.*, **64**, 393-406(2006).
20. J.P. Grist, and S.A. Josey, "Inverse analysis adjustment of SOC air-sea flux climatology using ocean heat transport and constraints." *J. Climate*, **20**, 3274-3295 (2003).
21. E. Kalnay and 21 co-authors, "The NCEP/NCAR 40-year reanalysis project." *Bull. Am. Meteorol. Soc.*, **77**, 437-471 (1996).
22. Yu. Lisan, R.A. Weller and B. Sun, "Improving latent and sensible heat flux estimates for the Atlantic Ocean (1988-1999) by a synthesis approach." *J. Climate*, **17**, 373-393 (2004).
23. F. J. Wentz, C. Gentemann, D. Smith and D. Chelton, "Satellite measurements of sea surface temperature through clouds." *Science*, **288**, 847-850 (2000).
24. V.S.N. Murty, Y.V.B. Sarma and D. P. Rao, "Variability of oceanic boundary layer characteristics in the northern Bay of Bengal during MONTBLEX-90," *Proc. Ind. Acad. Sci. (Earth Planet. Sci.)*, **105(1)**, 41-61(1996).
25. N. Ducet, P.Y. Le Traon and G. Reverdine, "Global high-resolution mapping of ocean circulation from the combination of T/P and ERS-1/2." *J. Geophys. Res.*, **105**, 19477-19498 (2000).
26. O. M. Smedstad, H. E. Hurlburt, E. J. Metzer, R. C. Rhodes, J. F. Shiriver, A. J. Walcraft and A. B. Kara, "An operational eddy resolving 1/16° global nowcast/forecast system." *J. Mar. Sys.*, **40**, 341-361 (2003).
27. W. J. Emery and R. E. Thomson, *Data analysis methods in Physical Oceanography*. Second and Revised Edition, Elsevier, New York, 638 pp (2001).
28. J.G. Colborn, *Thermal structure of the Indian Ocean*. IIOE Monograph 2, An East-West Press, 175 pp (1975).
29. F. Durand, S.R. Shetye, J. Vialard, D. Shankar, S.S.C. Shenoi, C. Ethe and G. Madec, "Impact of temperature inversions on SST evolution in the southeastern Arabian Sea during the pre-summer monsoon seasons." *Geophys Res Lett.*, **31**, L01305, doi:10.1029/2003GL018906 (2004).
30. D. Shankar, V.V. Gopalakrishna, S.S.C. Shenoi, F. Durand, S. R. Shetye, C. K. Rajan, Z. Johnson, N. Araligidad and G. S. Michael, "Observational evidence for westward propagation of temperature inversions in the southeastern Arabian Sea." *Geophys. Res. Lett.*, **31,** doi:10.1029/2004GL019652(2004).
31. N.H. Saji, B. N. Goswami, P. N. Vinaychandran and T. Yamagata, "A dipole mode in the tropical Indian Ocean." *Nature*, **401**, 360-363 (1999).
32. P.J. Webster, A. M. Moore, J. P. Loschnigg and R. R. Leben, "Coupled ocean-atmosphere dynamics in the Indian Ocean during 1997-98." *Nature*, **401**, 356-360 (1999).
33. R.A. Madden and P. R. Julian, "Description of global scale circulation cells in the tropics with a 40-50 day period." *J. Atmos. Sci.*, **29**, 1109-1123 (1972).
34. G.S. Bhat, Prashanth L. Rao, V.G. Sangolli, G.P. Bhat, A. B. Chandelkar, H. Rao and V.B. Kadav, "Diurnal and intraseasonal variations observed on the west coast of India." *Mausam*, **56 (1)**, 97-106(2005).